

INFLUENCE OF CURRENT DENSITY ON MORPHOLOGY AND ROUGHNESS OF SONOELECTRODEPOSITED Zn-Co-Al₂O₃ NANOCOMPOSITE COATINGS

Dragana Kostić¹, Marija Mitrović^{1*}, Milorad Tomić^{1,3}, Regina Fuchs – Godec², Duško Kostić¹

¹ University of East Sarajevo, Faculty of Technology, Karakaj, Zvornik, Republic of Serbia, B&H

² University of Maribor, Faculty of Chemistry and Chemical Technology, Maribor, Slovenia

³ Engineering Academy of Serbia, Belgrade, Serbia

* Corresponding author: marija.ridjovic@tfzv.ues.rs.ba

Abstract: Nanocomposite Zn-Co-Al₂O₃ coatings were electrodeposited from three different solutions, at 1, 2, 4 and 6 A/dm² current densities. Electrodeposition time was same for all samples, 15 minutes. Steel plates were used as cathodes while the anode was made of 99.99% pure zinc. All samples were mechanically and chemically prepared before electrochemical deposition of the Zn-Co-Al₂O₃ nanocomposite coating. Electroplating solutions were prepared from the chemicals of p.a. purity and aluminium oxide nanoparticles. All solutions possessed the same chemical composition, they differed only in the concentration of Al₂O₃. Solution R1 was without Al₂O₃, while solutions R2 and R3 contained 2 g/dm³ and 5 g/dm³ Al₂O₃, respectively. All experiments were performed in an electrochemical cell, with a volume of 100 cm³ at room temperature and atmospheric pressure. The surface of the obtained coatings was examined by Leica EZ4 HD optical microscope at a 100x magnification, while the roughness was measured by TR200 device. Based on the obtained results, it can be concluded that the thickness of the obtained Zn-Co-Al₂O₃ coatings depends on the current density, but also on the composition of the solution. With increasing current density, the thickness of the coating increases, as well as the roughness of the deposited coatings, while the current utilization decreases with increasing current density, no matter of plating solution composition. The morphology of the coatings was generally uniform and compact with good adhesion

Keywords: nanocomposite coatings, electrochemical deposition, roughness, ultrasonic agitation.

1. INTRODUCTION

Electrodeposition stands as a versatile and economical approach for producing an extensive range of 2D and 3D materials, including coatings and films. The principles of the electrodeposition process are based on the electrochemical phenomena associated with the reduction of electroactive and accompanying species on the cathode surface. Over the past twenty years, the process of electrodeposition for composite coatings has garnered significant attention from the scientific community. This heightened interest stems from the potential of such coatings to exhibit exceptional properties, thereby opening the

door to a wide array of diverse applications. Various routes exist for producing composite materials; however, electrodeposition presents distinct advantages. It enables precise regulation of deposition rate, i.e. coating thickness, composition, and final properties of deposit. Moreover, electrodeposition holds a cost advantage over other composite manufacturing techniques. Composite coatings consist of a matrix enhanced with a secondary phase. This matrix, serving as the core structure, can be a metal, alloy, conductive polymer, or conductive ceramic. On the other hand, the second phase introduces an additional dimension to the composition, taking the form of particles, fibers, or whiskers, each contributing to the coating's

distinct properties. Thus, in literature can be found a different combination of composite coatings, such are polymer matrix – ceramic particles, metal – polymer sandwich layers or nanostructured deposits [1-13]. The particles embedded within the matrix can assume a wide array of shapes, ranging from spheroidal and acicular to plate-like or layered structures. The particles used as a second phase in literature had broad size spectrum, extending from submillimeter down to several nanometers. A different salts and oxides are introduced in zinc matrix in order to produce the zinc composite coatings, like TiO_2 [14], SiC [15], CeO_2 [16-18], YSZ [19], Al_2O_3 [20], CNT [21], SiO_2 [22] etc. When it comes to the zinc alloys as a matrix, the most examined one is Zn-Ni. Although numerous composite coatings have been explored through the electrodeposition route, each composite system presents its own set of challenges. Factors such as the stability of plating solutions, the method of agitation, the quantity of the second phase, temperature control, current density, and distribution, as well as the potential utilization of additives, all warrant careful consideration. The objective of this study is straightforward: to achieve a one-step electrodeposition process for producing Zn-Co- Al_2O_3 nanocomposite coatings and subsequently examination of their properties. As far as the authors are aware, there is currently a lack of existing reports concerning this specific category of composite coatings.

2. MATERIALS AND METHODS

To facilitate the deposition of the Zn-Co- Al_2O_3 composite coating, a steel plate (dimensions $3.0 \times 3.0 \times 0.1$ cm) was employed as the working electrode. The anode was made of 99.99% pure zinc. Prior to the coating deposition process, the cathode surface underwent the following preparation steps:

1. mechanical grounding with #500, #900, #1200, and #2000 emery paper;
2. degreasing using detergent;
3. rinsing with both, tap and distilled water;
4. chemical degreasing in a solution composed of: 35g/dm^3 NaOH, 45g/dm^3 Na_2CO_3 and 4g/dm^3 $\text{Na}_3\text{PO}_4 \times 10\text{H}_2\text{O}$, at a temperature of 85°C for 15 minutes;
5. rinsing both tap and distilled water;
6. etching in a 20% H_2SO_4 solution at 65°C for 60 seconds;
7. rinsing with both, tap and distilled water.

Subsequently, the prepared steel samples (acting as cathodes) were utilized for the galvanostatic deposition of composite coatings. This process was conducted at room temperature using varying current densities of 1, 2, 4, and 6A/dm^2 . The electrochemical cell had a volume of 0.1dm^3 . The coating deposition was performed from chloride plating solutions, as detailed in Table 1. The experiments were conducted under ultrasonic agitation generated by ultrasound bath. The electrodeposition cell were placed in the middle of ultrasound bath to obtain the uniform distribution of ultrasound throughout the plating solution. All chemicals were p.a. purity and used as received. The size of the used alumina particles was $< 50\text{nm}$, obtained by transmission electron microscopy, according to Sigma Aldrich manufacturer.

Table 1. Composition of used plating solutions and working conditions

Compound	Concentration (mol/dm ³)		
	R1	R2	R3
KCl	3	3	3
H_3BO_3	0.8	0.8	0.8
ZnCl_2	0.1	0.1	0.1
$\text{CoCl}_2 \cdot 6\text{H}_2\text{O}$	0.03	0.03	0.03
Al_2O_3 (g/dm ³)	-	2	5
Working conditions	» current density: 1; 2; 4 и 6A/dm^2 » room temperature » ultrasound bath as a source of ultrasound		

The composition of the substrate and composite coatings was determined by energy dispersive X-ray spectroscopy, EDX8000, Shimadzu Instruments. By comparing the mass of the substrate before and after electrodeposition, and in accordance with Faraday's laws of electrolysis, the thickness of the coating and current density utilization were ascertained. The adhesion and coverage of the sonoelectrodeposited Zn-Co- Al_2O_3 composite coatings were examined by optical microscopy Leica E34 HD. The coatings roughness was studied by TR200 device, on a 0.8mm long measurement path at three different places.

3. RESULTS AND DISCUSSION

3.1. Composition of the substrate and deposited coatings

As mentioned in Materials and method section, the composition of the Fe substrate, Zn-Co and Zn-Co-Al₂O₃ composite coatings was determined by energy dispersive X-ray spectroscopy method. The chemical composition of the substrate is presented in Table 2.

Table 2. Chemical composition of Fe substrate used as cathode for the electrodeposition

Element	Weight percentage (%)
Fe	99,455
Mn	0,347
Cu	0,097
Au	0,064
V	0,037

The determined chemical compositions of obtained coatings are presented in Table 3.

Based on the provided data (Table 3), it can be observed that using the EDX device, the presence of Al₂O₃ nanoparticles was detected only in the coating deposited from solution R3 at a current density of 6 A/dm² under ultrasonic agitation. It is possible that particles are incorporated, but due to small size and amount it is difficult to be determined by used device. The content of Co in the coating increases with the augmentation of current density during the deposition of coatings from all three utilized solutions. The interesting result is increase in Co content in the coatings deposited at higher current densities from the solution containing particles. The deter-

mined amount of the Co in the coatings is still below the compositional reference line (CRL), so the Zn-Co is deposited anomalously, which implies that presence of the particles did not change the deposition mechanism. However, the explanation behind the increased deposition of Co in coatings derived from particle-containing solutions is likely due to the adsorption of metal ions onto the particle surfaces. This phenomenon enhances the mass transport of these ions compared to the diffusion of non-adsorbed metal ions.

Figure 1 provides a graphical illustration of the correlation between the thickness of the Zn-Co-Al₂O₃ composite coating and the applied current density for coatings deposited under ultrasonic agitation conditions. Meanwhile, Figure 2 illustrates the fluctuation in current density utilization as a function of the employed deposition current density for fabricating composite coatings from solutions R1-R3.

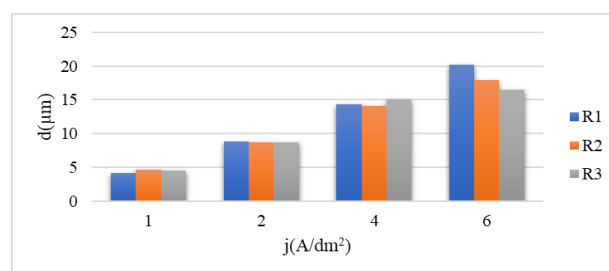


Figure 1. The dependence of coatings thickness on deposition current density

It can be noticed that at lower current densities of 1, 2, and 4 A/dm², the measured coating thickness remains consistent across coatings deposited from all three solutions. However, this consistency does not hold for coatings deposited at a current density of 6 A/dm². Specifically, for coatings deposited at

Table 3. Chemical composition of coatings deposited from R1-R3 plating solutions at current densities of 1, 2, 4 i 6 A/dm²

j (A/dm ²)	RASTVORI								
	R ₁			R ₂			R ₃		
	%Zn	%Co	%Al	%Zn	%Co	%Al	%Zn	%Co	%Al
1	99.1	0.9	-	99.4	0.6	-	99.3	0.7	-
2	98.1	1.9	-	91.6	8.4	-	91.0	9.0	-
4	89.8	10.2	-	87.4	12.6	-	87.5	12.5	-
6	88.9	11.1	-	88.4	11.6	-	84.2	12.9	2.8

this higher current density, it becomes evident that the solution's composition impacts the coating thickness. Notably, an increase in the Al_2O_3 content within the solution corresponds to a reduction in the coating thickness.

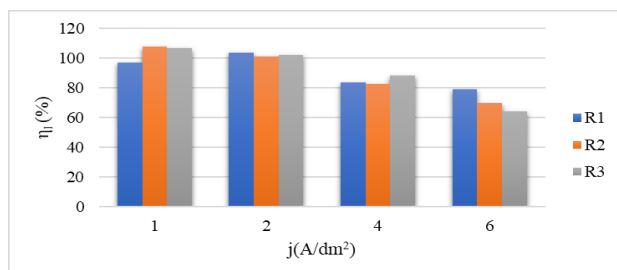


Figure 2. Influence of deposition current density on current density utilization

Figure 2 clearly shows that the utilization of current density per zinc decreases at current densities of 4 A/dm^2 ($\eta_i = 82.56\%$ to 88.05%) and 6 A/dm^2 ($\eta_i = 64.37\%$ to 78.77%). However, at current densities of 1 and 2 A/dm^2 , the current density utilization is greater than 96%. Interestingly, the calculated current density utilization exceeds 100% for coatings deposited at 1 and 2 A/dm^2 , based on the observed mass increase. This observation appears theoretically improbable. Nevertheless, a reasonable explanation could be the uniform incorporation of Al_2O_3 nanoparticles within the coating. Although these nanoparticles are too small to be detected by energy dispersive X-ray spectroscopy, their presence as a second phase could account for this phenomenon. It's also noteworthy that Al_2O_3 particles were

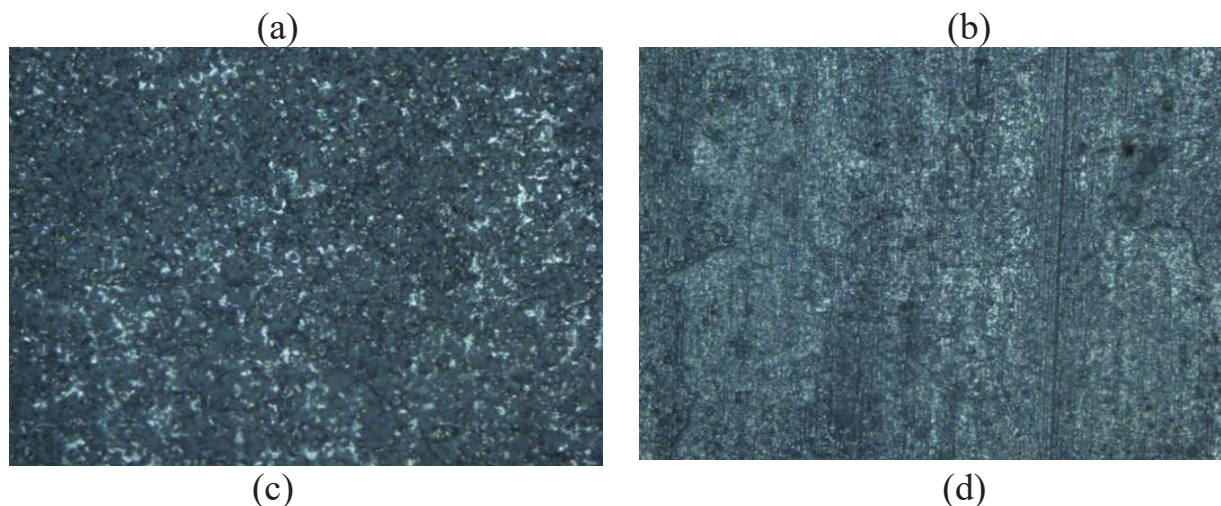


Figure 3. Surface of the $\text{Zn-Co-Al}_2\text{O}_3$ composite coatings deposited from plating solution R1 at current densities: a) 1 A/dm^2 , b) 2 A/dm^2 , c) 4 A/dm^2 u d) 6 A/dm^2 . Magnification 100x

successfully identified within the coating deposited at 6 A/dm^2 from solution R3 during ultrasonic mixing. This might be attributed to agglomeration of the nanoparticles during electrodeposition, rendering them detectable despite the lowest current utilization of 64.37%.

3.3. Coatings morphology

The surfaces of the samples were examined using an optical microscope. The recorded images of the coating surfaces from solutions R1-R3 at current

densities of 1, 2, 4, and 6 A/dm^2 are presented in Figures 3 to 5.

As evident from Figures 3 to 5, the coatings deposited at 1 A/dm^2 exhibit the most uniform and fine-grained morphology. The porosity becomes apparent in the coatings deposited at 2 A/dm^2 from a plating solution containing a second phase (Figure 2b and Figure 3b). Furthermore, it is evident that coatings deposited at 4 and 6 A/dm^2 possess a darker appearance (due to higher content of cobalt), with larger formed grains in comparison to coatings deposited at lower current densities.

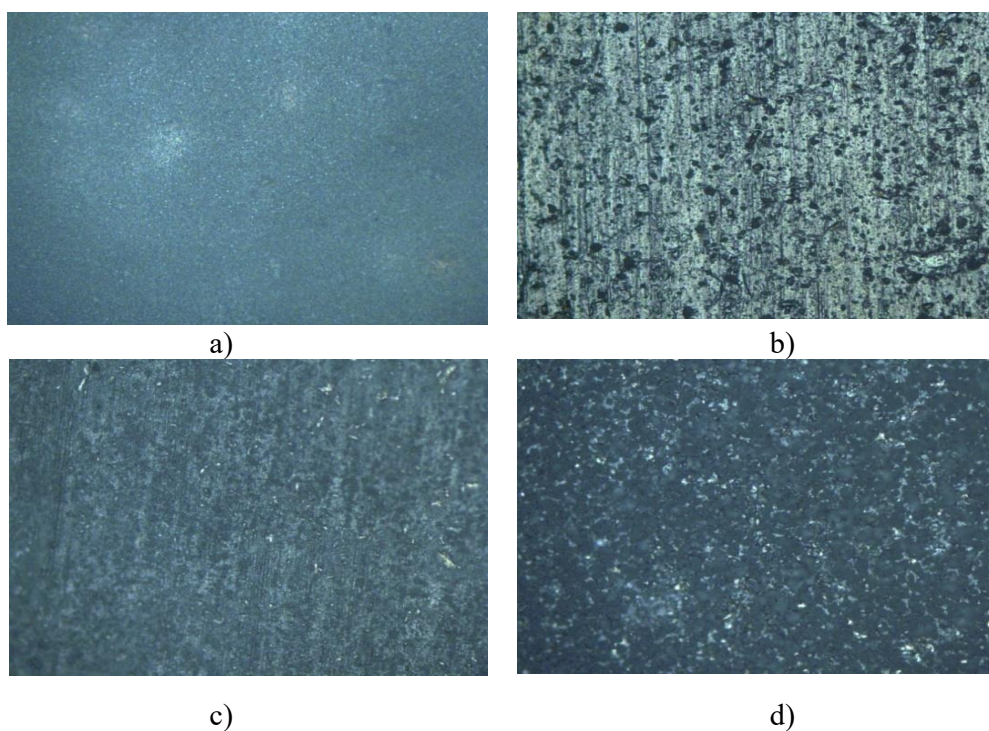


Figure 4. Surface of the Zn-Co- Al_2O_3 composite coatings deposited from plating solution R2 at current densities: a) $1\text{A}/\text{dm}^2$, b) $2\text{A}/\text{dm}^2$, c) $4\text{A}/\text{dm}^2$ u d) $6\text{A}/\text{dm}^2$. Magnification 100x

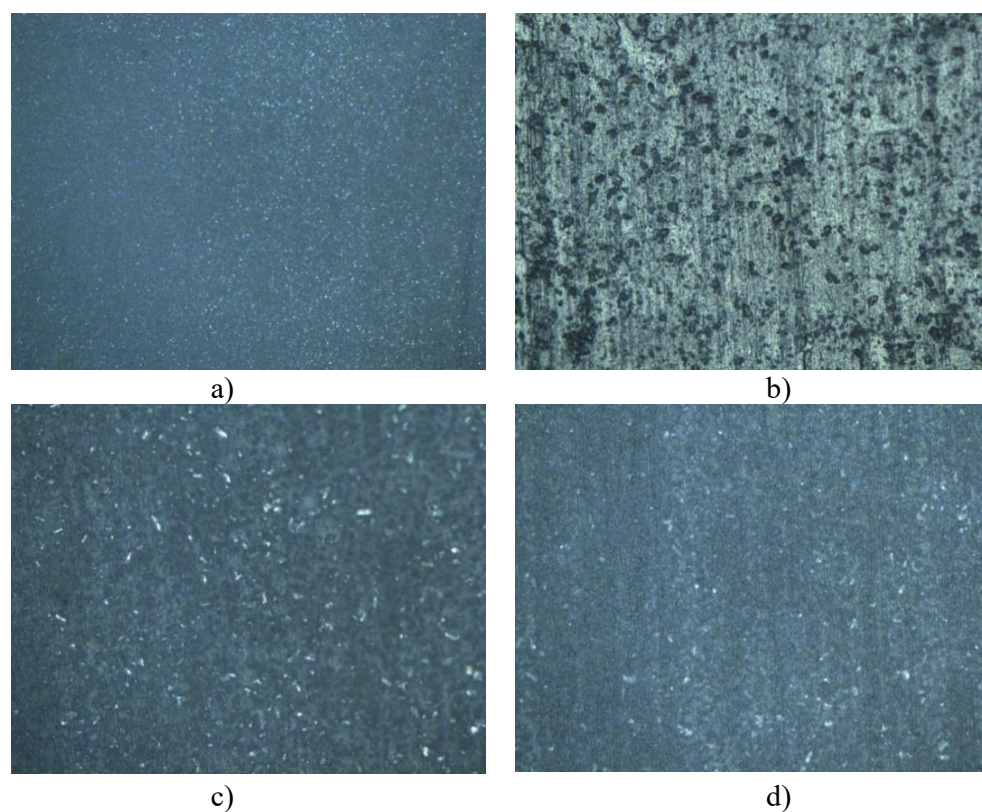


Figure 5. Surface of the Zn-Co- Al_2O_3 composite coatings deposited from plating solution R3 at current densities: a) $1\text{A}/\text{dm}^2$, b) $2\text{A}/\text{dm}^2$, c) $4\text{A}/\text{dm}^2$ u d) $6\text{A}/\text{dm}^2$. Magnification 100x

3.4. Coatings roughness

Table 4. exhibit measured roughness parameters of the Zn-Co-Al₂O₃ coatings electrodeposited from three different plating solutions and at current densities of 1A/dm², 2A/dm², 4 A/dm² and 6A/dm². The following roughness parameters are measured: Ra - arithmetic average height (average absolute deviation of the roughness irregularities from the mean line over one sampling length), Rq - root mean square roughness (standard deviation of the distribution of surface heights), Rz - ten-point height (the difference in height between the average of the five highest peaks and the five lowest valleys along the assessment length of the profile); Ry - largest peak

to valley height (the largest value of the maximum peak to valley height parameters along the assessment length); Rt - maximum height of the profile (the vertical distance between the highest peak and the lowest valley along the assessment length of the profile); Rp - maximum height of peaks (the maximum height of the profile above the mean line within the assessment length); Rm - maximum depth of valleys (the maximum depth of the profile below the mean line within the assessment length); S - mean spacing of adjacent peaks (the average spacing of adjacent local peaks of the profile measured along the assessment length); Sm - mean spacing at mean line (the mean spacing between profile peaks at the mean

Table 4. The roughness parameters determined for the Zn-Co-Al₂O₃ coatings electrodeposited from three different plating solutions and at current densities of 1A/dm², 2A/dm², A/dm² and 6A/dm²

Roughness parameters	Solution											
	R1				R2				R3			
	Current density <i>j</i> (A/dm ²)											
	1	2	4	6	1	2	4	6	1	2	4	6
Ra(μm)	0.955	1.027	2.019	1.372	1.028	1.783	2.794	2.702	1.000	1.434	2.234	1.904
Rq(μm)	1.181	1.307	2.743	1.785	1.413	2.658	3.655	3.405	1.254	1.835	2.798	2.357
Rz(μm)	3.412	4.205	10.10	6.524	3.654	8.245	11.62	10.97	3.740	6.111	10.13	7.610
Ry(μm)	5.667	6.500	15.610	9.395	6.920	15.35	18.51	16.18	6.012	9.604	14.86	10.38
Rt(μm)	8.460	8.539	24.790	12.89	17.52	19.78	28.26	21.54	7.599	13.89	18.65	12.73
Rp(μm)	2.892	3.267	8.012	5.795	2.912	9.352	10.09	8.495	2.776	4.636	7.384	5.584
Rm(μm)	2.776	3.232	7.604	3.599	4.007	6.007	8.420	7.691	3.236	4.967	7.480	4.803
S(mm)	0.0888	0.0571	0.0701	0.0481	0.1538	0.0816	0.0769	0.0493	0.0481	0.0754	0.0547	0.0373
Sm(mm)	0.1538	0.0909	0.0888	0.0714	0.3076	0.1176	0.1052	0.0784	0.0952	0.1481	0.0701	0.0689
Sk	-0.074	-0.296	1.125	1.108	-1.784	0.896	0.756	0.221	-0.234	-0.374	-0.074	0.500

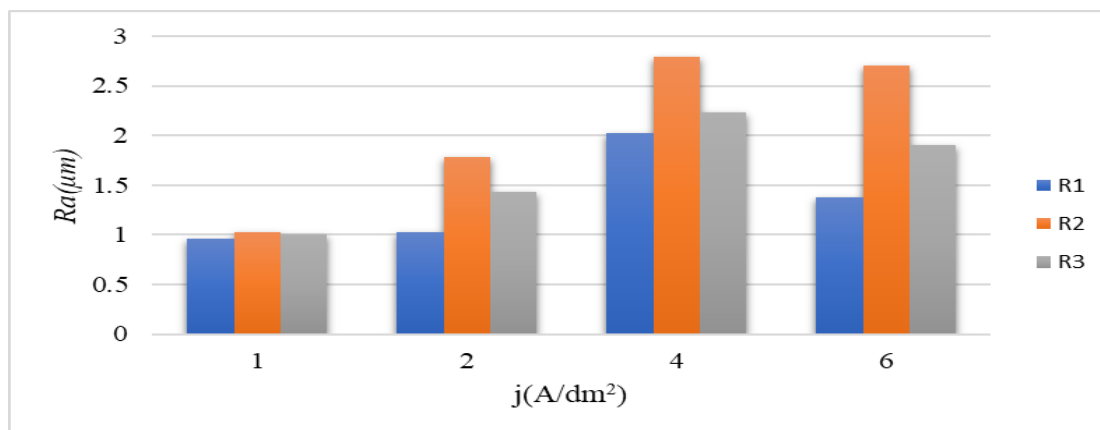


Figure 6. Dependence of determined Ra values on deposition current density

line); Sk - skewness factor of the profile (the third central moment of profile amplitude probability density function, measured over the assessment length).

Each of these parameters signifies a distinct property of the surface, potentially holding significance for specific applications. When assessing the roughness of electrodeposited coatings, the Ra parameter stands out as the commonly measured and discussed metric. The acquired Ra values for the deposited coatings are presented in Figure 6.

Clearly, the surface roughness parameter Ra demonstrates significant trends in response to varying current densities and distinct solution compositions. Notably, the highest Ra value, measuring 2.794 μm, is observed when employing solution R2 at a current density of 4 A/dm². In contrast, the lowest Ra value of 0.955 μm is documented for solution R1 at a current density of 1 A/dm². Furthermore, a consistent pattern emerges where elevating the current density across all solutions results in an increased Ra magnitude, particularly evident at current density levels of 1 A/dm², 2 A/dm², and 4 A/dm². Nevertheless, a noticeable deviation is observed at a current density of 6 A/dm², where the measured Ra values exhibit a decrease for coatings deposited from all solutions when compared to measurements taken at 4 A/dm². Of special interest is the observation that coatings deposited from solution R1, without Al₂O₃, exhibit the lowest surface roughness across all current density ranges. This observation implies that the presence of the particles contributes to the heightened roughness observed in the resulting coatings.

4. CONCLUSIONS

Based on the presented results obtained through electrochemical deposition and characterization of nanocomposite Zn-Co-Al₂O₃ coatings, several conclusions can be drawn. At lower current densities of 1, 2, and 4 A/dm², the measured coating thickness is approximately the same for coatings deposited from all three solutions, which is not the case for coatings deposited at a current density of 6 A/dm². For coatings deposited at a current density of 6 A/dm², it is evident that the solution composition affects the coating thickness, specifically, an increase in Al₂O₃ content in the solution results in a decrease in coating thickness. The zinc current density utilization decreases at deposition current densities of 4 A/dm² and 6 A/dm², while at deposition

current densities of 1 and 2 A/dm², the zinc current density utilization is above 96%. The finest-grained coatings are obtained when deposited at a current density of 1 A/dm². At a current density of 2 A/dm² in solutions containing Al₂O₃, weak coverage of the substrate is observed, while at current densities of 4 and 6 A/dm², significantly darker and coarser-grained coatings are obtained. Increasing the current density in all solutions also increases the Ra (surface roughness) value for current density values of 1, 2, and 4 A/dm². However, at a current density of 6 A/dm², the Ra value decreases for all solutions compared to the values measured at 4 A/dm². The lowest roughness is measured for coatings deposited from solution R1, which does not contain Al₂O₃ at any current density. It can be concluded that the presence of Al₂O₃ in the solution increases the roughness of the deposited coatings. Based on the morphological characteristics and measured roughness, it can be concluded that the most homogeneous and compact Zn-Co and nanocomposite Zn-Co-Al₂O₃ coatings are obtained at a current density of 1 A/dm² from all three utilized solutions.

5. LITERATURE

- [1] M. Jung, G. Lee, J. Choi, *Electrochemical plating of Cu-Sn alloy in non-cyanide solution to substitute for Ni undercoating layer*, *Electrochimica Acta*, 241 (2017) 229–236.
- [2] A. N. Murashkevich, O. A. Alisienok, I. M. Zharskii, E. V. Korobko, Z. A. Novikova, *The effect of the synthesis conditions of aluminum-modified nanosized titanium dioxide on the efficiency of its use in electrorheological dispersions*, *Colloid Journal*, 79 (1) (2017) 87–93.
- [3] M. K. Camargo, I. Tudela, U. Schmidt, A. J. Cobley, A. Bund, *Ultrasound assisted electrodeposition of Zn and Zn-TiO₂ coatings*, *Electrochimica Acta*, 198 (2016) 287–295.
- [4] J. M. Costa, A. F. de Almeida Neto, *Ultrasound-assisted electrodeposition and synthesis of alloys and composite materials: A review*, *Ultrasonic Sonochemistry*, 68 (2020) 105193.
- [5] S. K. Kim, H. J. Yoo, *Formation of bilayer Ni-SiC composite coatings by electrodeposition*, *Surface and Coating Technology*, 108–109 (1998) 564–569.

- [6] C. T. J. Low, R. G. A. Wills, F. C. Walsh, *Electrodeposition of composite coatings containing nanoparticles in a metal deposit*, Surface and Coating Technology, 201 1–2 (2006) 371–383.
- [7] M. Musiani, *Electrodeposition of composites: an expanding subject in electrochemical materials science*, Electrochimica Acta, 45 20 (2000) 3397–3402.
- [8] A. F. Zimmerman, G. Palumbo, K. T. Aust, U. Erb, *Mechanical properties of nickel silicon carbide nanocomposites*, Materials Science and Engineering: A, 328 1–2 (2002) 137–146.
- [9] N. S. Qu, K. C. Chan, D. Zhu, *Pulse co-electrodeposition of nano Al₂O₃ whiskers nickel composite coating*, Scripta Materialia, 50 8 (2004) 1131–1134.
- [10] N. Guglielmi, *Kinetics of the Deposition of Inert Particles from Electrolytic Baths*, Journal of Electrochemical Society, 119 8 (1972) 1009.
- [11] T. W. Clyne, P. J. Withers, “An Introduction to Metal Matrix Composites,” *An Introduction to Metal Matrix Composites*, Jun. 1993, doi: 10.1017/CBO9780511623080.
- [12] M. Pavlović, *Korozija i zaštita materijala*. Beograd: Tehnički fakultet Bor, 2012.
- [13] A. R. Despic, K. I. Popov, *Transport-controlled deposition and dissolution of metals*, Modern Aspects of Electrochemistry, 7 (1972) 199–313.
- [14] T. Frade, V. Bouzon, A. Gomes, M.I. da Silva Pereira, *Pulsed-reverse current electrodeposition of Zn and Zn-TiO₂ nanocomposite films*. Surface and Coatings Technology 204 21-22 (2010) 3592-3598.
- [15] M. Sajjadnejad, A. Mozafari, H. Omidvar, M. Javanbakht, *Preparation and corrosion resistance of pulse electrodeposited Zn and Zn-SiC nanocomposite coatings*, Applied Surface Science 300 (2014) 1-7.
- [16] M. Ridošić, M. Bučko, A. Salicio-Paz, E. García-Lecina, Lj. Živković, J. Bajat, *Ceria particles as efficient dopant in the electrodeposition of Zn-Co-CeO₂ composite coatings with enhanced corrosion resistance: The effect of current density and particle concentration*, Molecules 26(15) (2021) 4578.
- [17] M. Ridošić, A. Salicio-Paz, E. Garcia-Lecina, P. Zabinski, Lj. Živković, J. Bajat, *The effect of the ultrasound agitation and source of ceria particles on the morphology and structure of the Zn-Co-CeO₂ composite coatings*. Journal of materials research and technology 13 (2021) 1336-1349.
- [18] M. Ridošić, N.D. Nikolić, A. Salicio-Paz, E. García-Lecina, Lj. Živković, J. Bajat, *Zn-Co-CeO₂ vs. Zn-Co Coatings: Effect of CeO₂ Sol in the Enhancement of the Corrosion Performance of Electrodeposited Composite Coatings*. Metals, 11(5) (2021) 704.
- [19] X. Xia, I. Zhitomirsky, J.R. McDermid, *Electrodeposition of zinc and composite zinc-yttria stabilized zirconia coatings*. Journal of materials processing technology 209(5) (2009) 2632-2640.
- [20] M.V. Tomić, M.G. Mitrović, *Electrodeposition of Zn-Mn/CeO₂ composite coatings: evaluation of corrosion properties*. Journal of Solid State Electrochemistry (2023) 1-10.
- [21] B.M. Praveen, T.V. Venkatesha, *Electrodeposition and properties of Zn-Ni-CNT composite coatings*. Journal of alloys and compounds, 482(1-2) (2009) 53-57.
- [22] T.J. Tuaweri, G.D. Wilcox, *Behaviour of Zn-SiO₂ electrodeposition in the presence of N,N-dimethyldodecylamine*, Surface and Coatings Technology, 200 (20-21) (2006) 5921-5930.

УТИЦАЈ ГУСТИНЕ СТРУЈЕ НА МОРФОЛОГИЈУ И ХРАПАВОСТ Zn-Co-Al₂O₃ НАНОКОМПОЗИТНИХ ПРЕВЛАКА ТАЛОЖЕНИХ ПРИ УЛТРАЗВУЧНОМ МИЈЕШАЊУ

Сажетак: Наноконтропозитне превлаке Zn-Co-Al₂O₃ су добијене електрохемијским поступком таложења из три раствора различитог састава, при густинама струје 1, 2, 4 и 6А/dm² у трајању од 15 минута. Као катоде су коришћене челичне плочице, док је анода била од цинка чистоће 99,99%. Сви узорци су механички и хемијски припремани прије електрохемијског таложења наноконтропозитних Zn-Co-Al₂O₃ превлака. Коришћене хемикалије за растворе за таложење биле су п.а. чистоће. Сви раствори су били истог хемијског састава, разликовали су се само у концентрацији Al₂O₃. Раствор Р1 био је без Al₂O₃ наночестица, док су раствори Р2 и Р3 садржали 2g/dm³, односно 5g/dm³ Al₂O₃. Сви експерименти су извођени у електрохемијској ћелији, запремине 100cm³ на собној температури и атмосферском притиску. Површине добијених превлака снимане су оптичким микроскопом Leica EZ4 HD на увећању од 100 пута, док је хрпавост мјерена на уређају TR200. На основу добијених резултата закључено је да дебљина добијених превлака Zn-Co-Al₂O₃ зависи од густине струје, али и од састава раствора. Код сва три коришћена раствора са повећањем густине струје повећавала се дебљина превлаке, као и хрпавост исталожених превлака, док је искоришћење струје опадало са повећањем густине струје. Помоћу оптичког микроскопа видјело се да су превлаке углавном компактне и да добро покривају површину.

Кључне ријечи: наноконтропозитне превлаке, електрохемијско таложење, хрпавост, ултразвучно мијешање.

Paper received: 30 August 2023

Paper accepted: 12 February 2024



This work is licensed under a Creative Commons Attribution-NonCommercial 4.0 International License